INTERNATIONAL JOURNAL FOR NUMERICAL METHODS IN FLUIDS, VOL. 26, 1–16 (1998)

# DEVELOPMENT AND ASSESSMENT OF A VARIABLE-ORDER NON-OSCILLATORY SCHEME FOR CONVECTION TERM DISCRETIZATION

A. VARONOS[1]* AND G. BERGELES[1]

[1] *Laboratory of Aerodynamics—Fluids Section, Department of Mechanical Engineering, National Technical University of Athens, 9 Heroon Polytechniou Avenue, 157-73 Athens, Greece*

## SUMMARY

A new scheme for convection term discretization is developed, called VONOS (variable-order non-oscillatory scheme). The development of the scheme is based on the behaviour of well-known non-oscillatory schemes in the pure convection of a step profile test case. The new scheme is a combination of the QUICK and BSOU (bounded second-order upwind) schemes. These two schemes do not have the same formal order of accuracy and for that reason the formal order of accuracy of the new scheme is variable. The scheme is conservative, bounded and accurate. The performance of the new scheme was assessed in three test cases. The results showed that it is more accurate than currently used higher-order schemes, so it can be used in a general purpose algorithm in order to save computational time for the same level of accuracy. © 1998 John Wiley & Sons, Ltd.

*Int. J. Numer. Meth. Fluids*, **26**: 1–16 (1998)

KEY WORDS: finite difference schemes; boundedness property; convection–diffusion problems

## 1. INTRODUCTION

In recent years the discussion concerning errors associated with the discretization of the convection terms of transport equations has led to the conclusion that the 'hybrid' difference scheme should no longer be used for convective modelling. Leonard and Drummond[1] stress the fact that the 'hybrid' scheme gives in some cases not only quantitative but also qualitative errors. However, the 'hybrid' scheme is very robust and, owing to the oscillatory behaviour of higher-order schemes, clear indication on the advantages of higher-order convective modelling was not conclusive.

The oscillatory behaviour of schemes such as second-order upwind (SOU) and QUICK[2] is related to the boundedness property. Both schemes are unbounded, i.e. in the absence of any source terms the internal grid node values do not remain between the maximum and minimum boundary values. A discussion concerning the boundedness mathematical and computational properties is given by Gaskell and Lau[3] and Pascau and Perez.[4] Several methods have been developed in order to bound

* Correspondence to: A. Varonos, Department of Mechanical Engineering, National Technical University of Athens, 9 Heroon Polytechniou Avenue, 157-73 Zografou, Athens, Greece.

Contract grant sponsor: EU/DG XII; Contract grant number: JOF-CT95-0005.

CCC 0271–2091/98/010001–16 $17.50 *Received July 1996*

higher-order schemes. The BSOU scheme[5] is a SOU scheme which blends the first-order upwind (FOU) scheme in the area where SOU is unbounded. The same is valid for the SMART scheme,[3] which is a bounded version of QUICK. NOTABLE[4] is another alternative for a higher-order bounded scheme. The formal accuracy of BSOU is second-order, whilst for QUICK and NOTABLE it is third-order. The formal order of accuracy of the difference scheme is the result of the higher-order truncation error analysis on uniform grids.

An important question now is whether the increase in the formal order of accuracy of the difference scheme gives more accurate results. It is clear that the formal order of accuracy of the scheme should not be confused with the results accuracy. The results accuracy is measured against an exact solution and is the main concern of convective modelling. Furthermore, it should also be noticed that the 'hybrid' scheme fails to describe accurately phenomena in which convection is dominant. In contrast, when strongly diffusive phenomena are present, the 'hybrid' scheme gives adequately accurate results.[1,5] For the above reasons the effect of the formal order of accuracy of the scheme must be studied by means of a convective problem with an analytical solution. A very extensive study has been carried out by Leonard.[6] There it is clear that the increase in the formal order of accuracy does not guarantee more accurate results. Therefore the behaviour of the scheme is not always proportional to its formal order of accuracy and it must always be studied before finally the scheme is implemented into the computational code.

The aim of this paper is to present step-by-step the development of a new bounded second/third-order-accurate scheme called VONOS (variable-order non-oscillatory scheme). The formulation given is directly applicable for incompressible flows. The scheme is based on the BSOU and QUICK schemes and its performance is assessed against the SMART and NOTABLE schemes in three test cases.

## 2. DEVELOPMENT OF VONOS

The general form of the transport equation of variable $\phi$ in a two-dimensional Cartesian co-ordinate system is

$$\frac{\partial}{\partial x}(\rho u\phi)+\frac{\partial}{\partial y}(\rho v\phi)-\frac{\partial}{\partial x}\left(\Gamma_\phi\frac{\partial\phi}{\partial x}\right)-\frac{\partial}{\partial y}\left(\Gamma_\phi\frac{\partial\phi}{\partial y}\right)=S_\phi, \tag{1}$$

where $u$ and $v$ are the velocities in the $x$- and $y$-direction respectively, $\Gamma_\phi$ is the diffusion coefficient and $S_\phi$ denotes the source term.

Equation (1) is discretized by integrating over the control volume shown in Figure 1. The integration yields

$$\left[\rho u\phi-\Gamma_\phi\frac{\partial\phi}{\partial x}\right]_{\mathrm{e}}\Delta y_{\mathrm{ns}}-\left[\rho u\phi-\Gamma_\phi\frac{\partial\phi}{\partial x}\right]_{\mathrm{w}}\Delta y_{\mathrm{ns}}+\left[\rho v\phi-\Gamma_\phi\frac{\partial\phi}{\partial y}\right]_{\mathrm{n}}\Delta x_{\mathrm{ew}}$$
$$-\left[\rho v\phi-\Gamma_\phi\frac{\partial\phi}{\partial y}\right]_{\mathrm{s}}\Delta x_{\mathrm{ew}}=S_\phi\cdot Vol, \tag{2}$$

where each quantity inside brackets is calculated on the corresponding face of the control volume.

The calculation of the derivatives associated with the diffusion terms is made by central differences, second-order-accurate, since the values of $\phi$ are known at the centre of the computational cells and no approximation is involved:

$$\left.\frac{\partial\phi}{\partial x}\right|_{\mathrm{e}}=\frac{\phi_{\mathrm{E}}-\phi_{\mathrm{P}}}{\Delta x_{\mathrm{EP}}}. \tag{3}$$

 

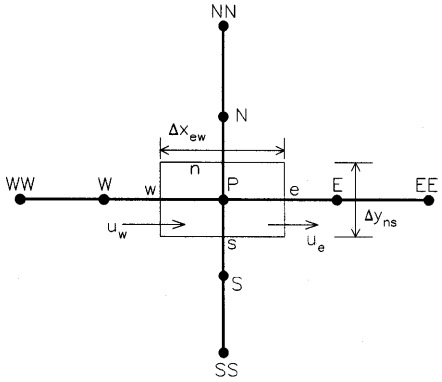


Figure 1. Control volume

The convective modelling deals with the approximation of the value of variable $\phi$ on the cell faces. The FOU and SOU schemes give

$$\phi_{\mathrm{e}}^{\mathrm{FOU}} = \begin{cases} \phi_{\mathrm{P}} & \text{if } u_{\mathrm{e}} > 0, \\ \phi_{\mathrm{E}} & \text{if } u_{\mathrm{e}} < 0, \end{cases} \tag{4}$$

$$\phi_{\mathrm{e}}^{\mathrm{SOU}} = \begin{cases} \phi_{\mathrm{P}} + \frac{1}{2}(\phi_{\mathrm{P}} - \phi_{\mathrm{W}}) & \text{if } u_{\mathrm{e}} > 0, \\ \phi_{\mathrm{E}} + \frac{1}{2}(\phi_{\mathrm{E}} - \phi_{\mathrm{EE}}) & \text{if } u_{\mathrm{e}} < 0. \end{cases} \tag{5}$$

For simplicity the expressions involved in the development of VONOS will be given for uniform grids only. The final formulation of the scheme will be generalized and include the necessary terms for non-uniform grids.

The study of the boundedness is made by means of a normalized variable diagram. Assuming that $u_{\mathrm{e}} > 0$, the normalized variable $\hat{\phi}$ is defined as

$$\hat{\phi}_k = \frac{\phi_k - \phi_{\mathrm{W}}}{\phi_{\mathrm{E}} - \phi_{\mathrm{W}}}, \quad k = W, w, P, e, E. \tag{6}$$

The normalized variable diagram presents the plane $[\hat{\phi}_{\mathrm{P}}, \hat{\phi}_{\mathrm{e}}]$ by the function $\hat{\phi}_{\mathrm{e}} = f(\hat{\phi}_{\mathrm{P}})$. The function $f$ is bounded when the following relations are valid.

(a) For $\hat{\phi}_{\mathrm{P}} \in [0,1]: f(\hat{\phi}_{\mathrm{P}}) \leqslant 1$ and $f(\hat{\phi}_{\mathrm{P}}) \geqslant \hat{\phi}_{\mathrm{P}}, f(0) = 0, f(1) = 1$.
(b) For $\hat{\phi}_{\mathrm{P}} \notin [0,1]: f(\hat{\phi}_{\mathrm{P}}) = \hat{\phi}_{\mathrm{P}}$.

The shaded area in Figure 2 and the line $\hat{\phi}_{\mathrm{e}} = \hat{\phi}_{\mathrm{P}}$ show the area where the boundedness condition is satisfied. In the same figure the FOU, SOU, QUICK and BSOU schemes are also presented. It is clear that the SOU and QUICK schemes are unbounded.

For completeness the normalized variable expressions for the FOU, SOU and QUICK schemes are given by

$$\hat{\phi}_{\mathrm{e}}^{\mathrm{FOU}} = \hat{\phi}_{\mathrm{P}}, \tag{7}$$

$$\hat{\phi}_{\mathrm{e}}^{\mathrm{SOU}} = 1{\cdot}5\hat{\phi}_{\mathrm{P}}, \tag{8}$$

$$\hat{\phi}_{\mathrm{e}}^{\mathrm{QUICK}} = \tfrac{3}{8}(1 + 2\hat{\phi}_{\mathrm{P}}). \tag{9}$$

 

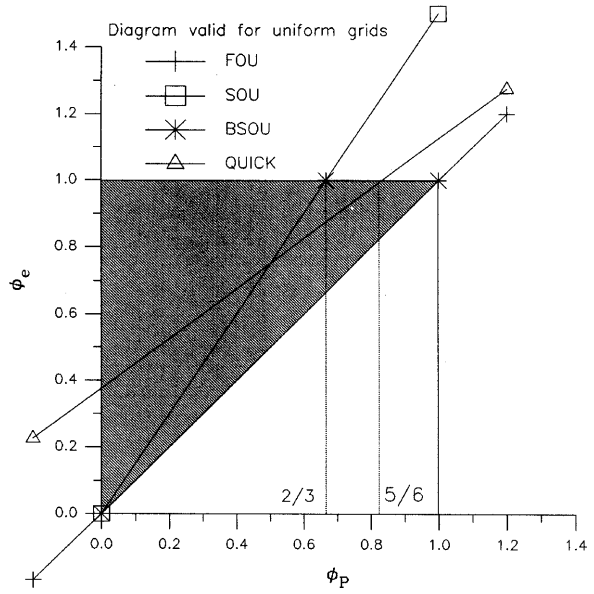


Figure 2. Convection boundedness criterion: FOU, SOU, BSOU and QUICK in normalized variable diagram

The procedure applied by Papadakis and Bergeles[5] led to the BSOU scheme

$$\hat{\phi}_e^{BSOU} = \begin{cases} \hat{\phi}_P & \text{for } \hat{\phi}_P < 0, \\ 1{\cdot}5\hat{\phi}_P & \text{for } 0 \leqslant \hat{\phi}_P < \frac{2}{3}, \\ 1 & \text{for } \frac{2}{3} \leqslant \hat{\phi}_P \leqslant 1, \\ \hat{\phi}_P & \text{for } \hat{\phi}_P > 1. \end{cases} \tag{10}$$

The NOTABLE scheme[4] is described by function

$$\hat{\phi}_e^{NOTABLE} = \begin{cases} \hat{\phi}_P(\hat{\phi}_P^2 - 2{\cdot}5\hat{\phi}_P + 2{\cdot}5) & \text{for } \hat{\phi}_P \in [0,1], \\ \hat{\phi}_P & \text{for } \hat{\phi}_P \notin [0,1] \end{cases} \tag{11}$$

and is unconditionally bounded (Figure 3).

Bounding now the QUICK scheme means that the function $f$ must cross the point (0,0) and that the part of the QUICK curve that exceeds $\hat{\phi}_e = 1$ is limited to $\hat{\phi}_e = 1$. The bounded QUICK scheme is the SMART scheme.[3] The point where QUICK crosses $\hat{\phi}_e = 1$ is $\hat{\phi}_P = \frac{5}{6}$. However, there are practically infinite alternatives to connect the point (0,0) with a point on the QUICK curve. In the present work this is done by means of the line $\hat{\phi}_e = 10\hat{\phi}_P$ as suggested by Leonard and Drummond.[1] Then the form of the SMART scheme becomes (Figure 3)

$$\hat{\phi}_e^{SMART} = \begin{cases} \hat{\phi}_P & \text{for } \hat{\phi}_P \notin [0,1], \\ 10\hat{\phi}_P & \text{for } 0 \leqslant \hat{\phi}_P < \frac{3}{74}, \\ \frac{3}{8}(1 + 2\hat{\phi}_P) & \text{for } \frac{3}{74} \leqslant \hat{\phi}_P \leqslant \frac{5}{6}, \\ 1 & \text{for } \frac{5}{6} \leqslant \hat{\phi}_P \leqslant 1. \end{cases} \tag{12}$$

SMART was tested in the pure convection of a step profile test case, presented in the next section. The SMART behaviour according to this test case showed that the curve area where $\hat{\phi}_P > \frac{5}{6}$ gives

 

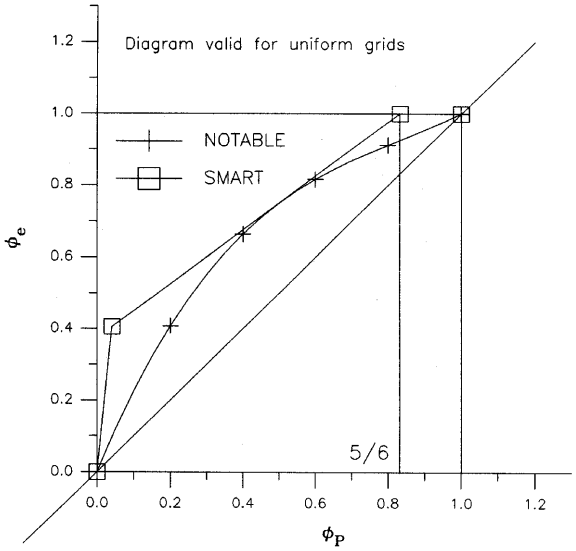


Figure 3. NOTABLE and SMART in normalized variable diagram

stability and convergence problems. This is also in accordance with the comments of Gaskell and Lau.[3] Of course, this statement should not be generalized for all flow configurations.

VONOS considers the fact that the QUICK scheme has stability problems even in the case where it is bounded in the region $\hat{\phi}_P \in [\frac{5}{6},1]$. As can be seen in Figure 2, QUICK and SOU cross each other at $\hat{\phi}_P = 0{\cdot}5$. For that reason the QUICK part of the curve is valid only between $\hat{\phi}_P = \frac{3}{74}$ and 0·5. The part of the curve for $\hat{\phi}_P > 0{\cdot}5$ is described by the corresponding part of the BSOU scheme. VONOS (Figure 4) is described by the function

$$\hat{\phi}_e^{\mathrm{VONOS}} = \begin{cases} \hat{\phi}_P & \text{for } \hat{\phi}_P \notin [0,1], \\ 10\hat{\phi}_P & \text{for } 0 \leqslant \hat{\phi}_P < \frac{3}{74}, \\ \frac{3}{8}(1+2\hat{\phi}_P) & \text{for } \frac{3}{74} \leqslant \hat{\phi}_P \leqslant 0{\cdot}5, \\ 1{\cdot}5\hat{\phi}_P & \text{for } 0{\cdot}5 \leqslant \hat{\phi}_P \leqslant \frac{2}{3}, \\ 1 & \text{for } \frac{2}{3} \leqslant \hat{\phi}_P \leqslant 1. \end{cases} \tag{13}$$

From equation (13) it is clear that the scheme does not have constant formal order of accuracy in the area of $\hat{\phi}_P = 0{\cdot}5$. The formal accuracy varies from third-order ($\hat{\phi}_P < 0{\cdot}5$, QUICK) to second-order ($\hat{\phi}_P > 0{\cdot}5$, SOU). For that reason the scheme was named VONOS (variable-order non-oscillatory scheme).

The coefficients that take into account the non-uniformity of the grid are now given assuming that $u_e > 0$:

$$\xi = \frac{\Delta x_{eP}}{\Delta x_{PW}}, \qquad r = \frac{\Delta x_{EP}}{\Delta x_{PW}}. \tag{14}$$

The coefficients $q_1$ and $q_2$ are related to the QUICK part of VONOS and have the form

$$q_1 = \frac{2+r}{4}, \qquad q_2 = \frac{2+r}{4(1+r)}. \tag{15}$$

 

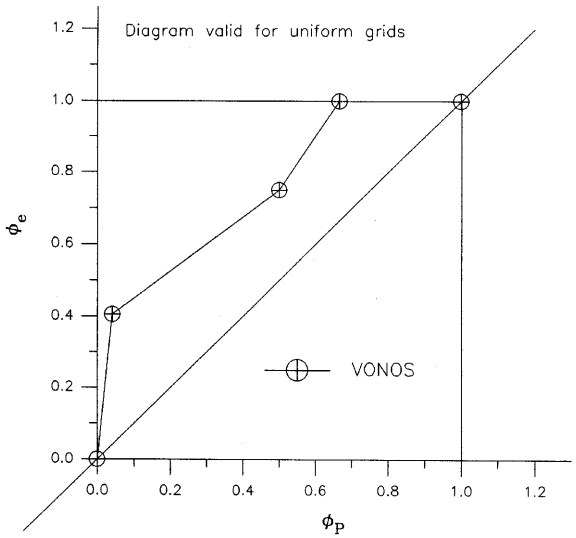


Figure 4. VONOS in normalized variable diagram

Then the general formulation of VONOS is

$$\hat{\phi}_e^{\mathrm{VONOS}} = \begin{cases} \hat{\phi}_P & \text{for } \hat{\phi}_P \notin [0,1], \\ 10\hat{\phi}_P & \text{for } 0 \leqslant \hat{\phi}_P < q_2/(10-q_1), \\ q_1\hat{\phi}_P + q_2 & \text{for } q_2/(10-q_1) \leqslant \hat{\phi}_P \leqslant q_2/(1+\xi-q_1), \\ (1+\xi)\hat{\phi}_P & \text{for } q_2/(1+\xi-q_1) \leqslant \hat{\phi}_P \leqslant 1/(1+\xi), \\ 1 & \text{for } 1/(1+\xi) \leqslant \hat{\phi}_P \leqslant 1. \end{cases} \tag{16}$$

As this scheme is non-linear, it is evident that an iterative process is required even for linear cases. The implementation of higher-order schemes into solvers for non-linear cases presents some difficulties, however. Although the schemes are bounded, their non-diffusive character can in some cases prohibit the total convergence of the solver. For that reason the downwind weighting factor *DWF* was proposed by Leonard and Mokhtari.[7] *DWF* is defined as

$$DWF = \frac{\phi_e - \phi_P}{\phi_E - \phi_P} = \frac{\hat{\phi}_e - \hat{\phi}_P}{1 - \hat{\phi}_P}, \tag{17}$$

and assuming that $u_e > 0$, we have $\phi_e = \phi_P + DWF(\phi_E - \phi_P)$. The application of this relation to equation (2) gives

$$A_P\phi_P = A_E\phi_E + A_W\phi_W + A_N\phi_N + A_S\phi_S + S_\phi \cdot Vol + SU_x + SU_y, \tag{18}$$

where

$$A_P = A_E + A_W + A_N + A_S,$$

$$A_E = \max(0, -CE) + DE, \qquad A_W = \max(0, CW) + DW,$$

$$\begin{aligned} SU_x = {} & \max(0, CE)DWF_e^+(\phi_P - \phi_E) + \max(0, -CE)DWF_e^-(\phi_P - \phi_E) \\ & + \max(0, CW)DWF_w^+(\phi_P - \phi_W) + \max(0, -CW)DWF_w^-(\phi_P - \phi_W), \end{aligned}$$

 

with

$$DE = [\Gamma_\phi]_e \frac{\Delta y_{ns}}{\Delta x_{EP}}, \qquad DW = [\Gamma_\phi]_w \frac{\Delta y_{ns}}{\Delta x_{PW}},$$

$$CE = [\rho u]_e \Delta y_{ns}, \qquad CW = [\rho u]_w \Delta y_{ns}.$$

The superscripts $+$ and $-$ on the downwind weighting factors indicate the direction of the $u$-velocity. The downwind weighting factors have to be calculated according to its sign.

The same relations expressed in the $y$-direction apply for the rest of the coefficients. In this way the system of equations can be solved by standard iterative techniques such as ADI. It should be noted that third-order schemes, when highly convective non-linear problems are concerned, may require the introduction of underrelaxation factors for the source terms $SU_x$ and $SU_y$.

Since the scheme involves five points in each direction ($x$ and $y$), the boundary nodes must be treated in a special way. In the present work the FOU approximation was applied to all boundaries. This was done for ease of implementation (simply by setting the downwind factor equal to zero) and because boundary conditions of higher order, although having increased accuracy, cause numerical instabilities.[8]

The performance of VONOS is assessed in the next section.

## 3. TEST CASES AND RESULTS

VONOS has been assessed in comparison with the NOTABLE and SMART schemes. The reason for this is that all three schemes are formally third-order-accurate. The two linear and the one non-linear cases that have been selected will provide information on the behaviour of each scheme and the advantages and disadvantages of the schemes' use in computational codes. The selected test cases are ones for which either analytic solutions or well-established results exist, so that the computational errors associated with the schemes can be directly calculated. Turbulent flow fields have not been simulated, in order to attribute any differences from the exact solutions to the properties of the numerical schemes.

### *3.1. Pure convection of a step profile*

This is a simple problem that is widely used for the characterization of convection difference schemes as diffusive or non-diffusive. It is the basis for the development of VONOS. This test problem simulates the case where two parallel streams of equal velocity but unequal $\phi$ (e.g. temperature) come into contact (Figure 5(a)). The diffusion coefficient is zero and the Reynolds number is infinite. Since there is no diffusion present, no mixing layer should form and the $\phi$ discontinuity should be maintained in the streamwise direction. This means that any mixing layer present in the solution is associated with the errors of the numerical scheme used.

Figures 5(b)–5(d) show the performance of NOTABLE, SMART and VONOS by comparison of the profiles at $x = 0{\cdot}5$ against the exact solution, using a uniform $21 \times 21$ Cartesian grid for three different angles $\theta = 25^\circ, 35^\circ$ and $45^\circ$ respectively. From these results it is clear that NOTABLE is the most diffusive scheme. SMART is less diffusive, but it cannot describe the discontinuity as accurately as VONOS. Since the three schemes are bounded, the solution does not present any overshoots or undershoots beyond the boundary values $\phi = 1$ and 2.

 

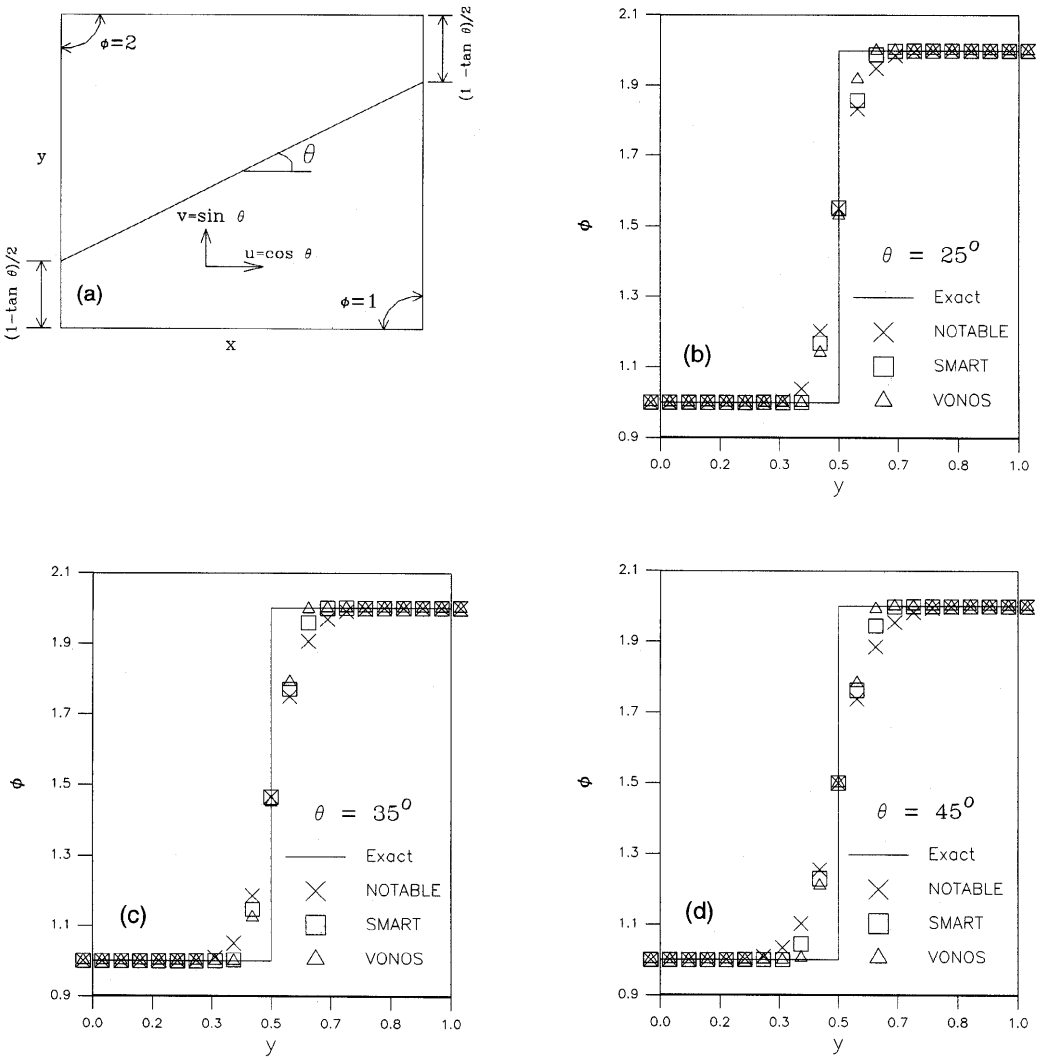


Figure 5. Pure convection of step profile: (a) boundary conditions; (b) $x=0{\cdot}5$, $=25°$; (c) $x=0{\cdot}5$, $\theta=35°$; (d) $x=0{\cdot}5$, $\theta=45°$

### 3.2. *Pure convection of a box profile*

This test case was investigated in order to assess the three schemes' performance in the calculation of a localized maximum in the transported profile. This test case was also selected so as to investigate the effect of grid refinement on the results of each scheme. The Reynolds number is again infinite. The flow angle to the horizontal direction is constant and equal to 45° (Figure 6(a)). This problem simulates, for example, the transport of the turbulence kinetic energy produced in a thin shear layer.

Figures 6(b)–6(d) show the results obtained with the three schemes at $x=0{\cdot}5$ for three different uniform computational grids $21\times21$, $31\times31$ and $41\times41$ respectively. These results indicate that VONOS describes better than NOTABLE and SMART the box profile. The NOTABLE scheme, although being formally third-order-accurate, presents important undershoots even in the $41\times41$ grid test.

 

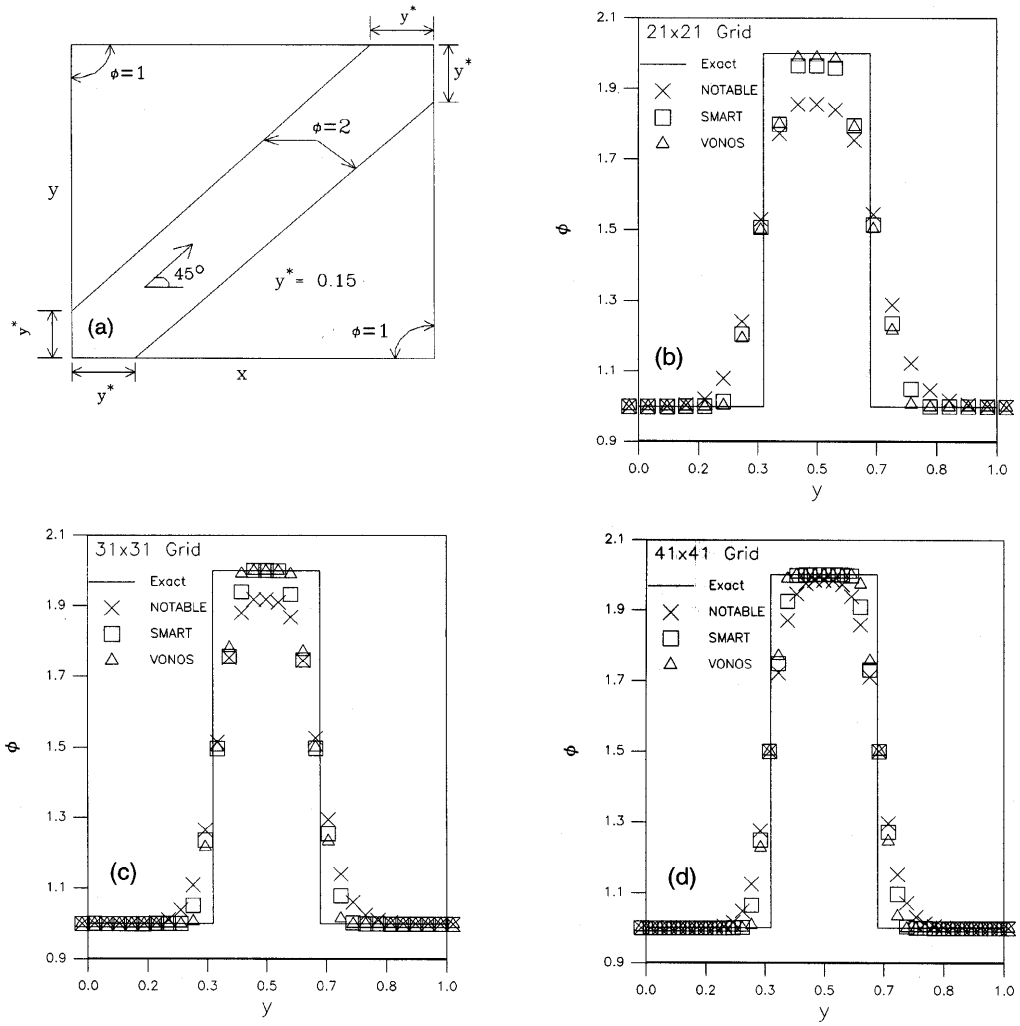


Figure 6. Pure convection of box profile: (a) boundary conditions; (b) $x=0{\cdot}5$, $21\times21$ grid; (c) $x=0{\cdot}5$, $31\times31$ grid; (d) $x=0{\cdot}5$, $41\times41$ grid

For test cases 3.1 and 3.2 the two convection equations were solved explicitly. An underrelaxation factor of 0·5 was necessary for VONOS and NOTABLE. The SMART scheme had convergence problems and an underrelaxation factor of 0·1 was employed in order to achieve fully converged solutions.

The effect of the flow angle $\theta$ (convection of a step profile) and grid refinement (convection of a box profile), given by the number of grid points in one direction, on the accuracy of NOTABLE, SMART and VONOS is shown in Figures 7 and 8 respectively. Accuracy is given by the % error between the numerical results and the exact solution for the $\phi$ distribution at $x=0{\cdot}5$. The % error is defined as

$$\%\text{error} = \frac{\sum_{i=2}^{N-1} \left|(\phi_{\text{exact}} - \phi_{\text{numerical}})/\phi_{\text{exact}}\right|}{N-2} \times 100, \tag{19}$$

 

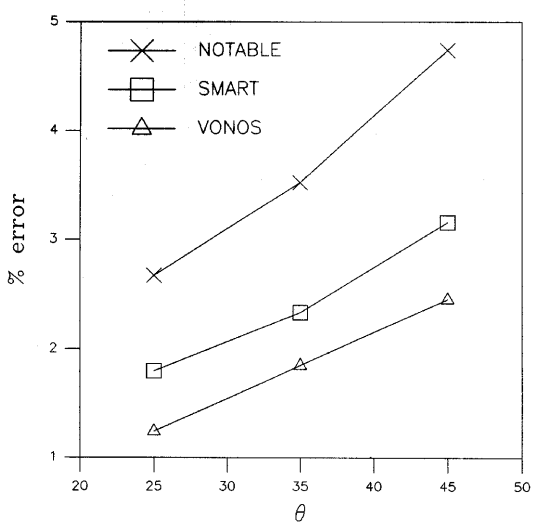


Figure 7. Effect of flow angle $\theta$ on accuracy of NOTABLE, SMART and VONOS (pure convection of step profile)

where $N$ is the number of grid points in the $y$-direction. The points $i = 1$ and $N$ have been excluded because they represent the boundary conditions. The points whose $y$ coincides with the location of discontinuities are also excluded, because the exact solution is not defined at these positions. From both figures it can be seen that VONOS always gives better results than NOTABLE and SMART.

### *3.3. Flow inside a lid-driven cavity*

The laminar recirculating flow inside a lid-driven cavity has been widely used for the assessment of numerical schemes. The reason for this is that the flow being laminar, there are no influences from the

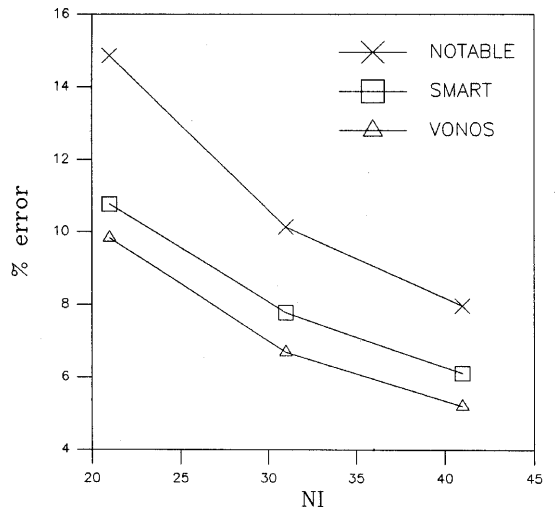


Figure 8. Effect of grid refinement (*NI*) on accuracy of NOTABLE, SMART and VONOS (pure convection of box profile)

 

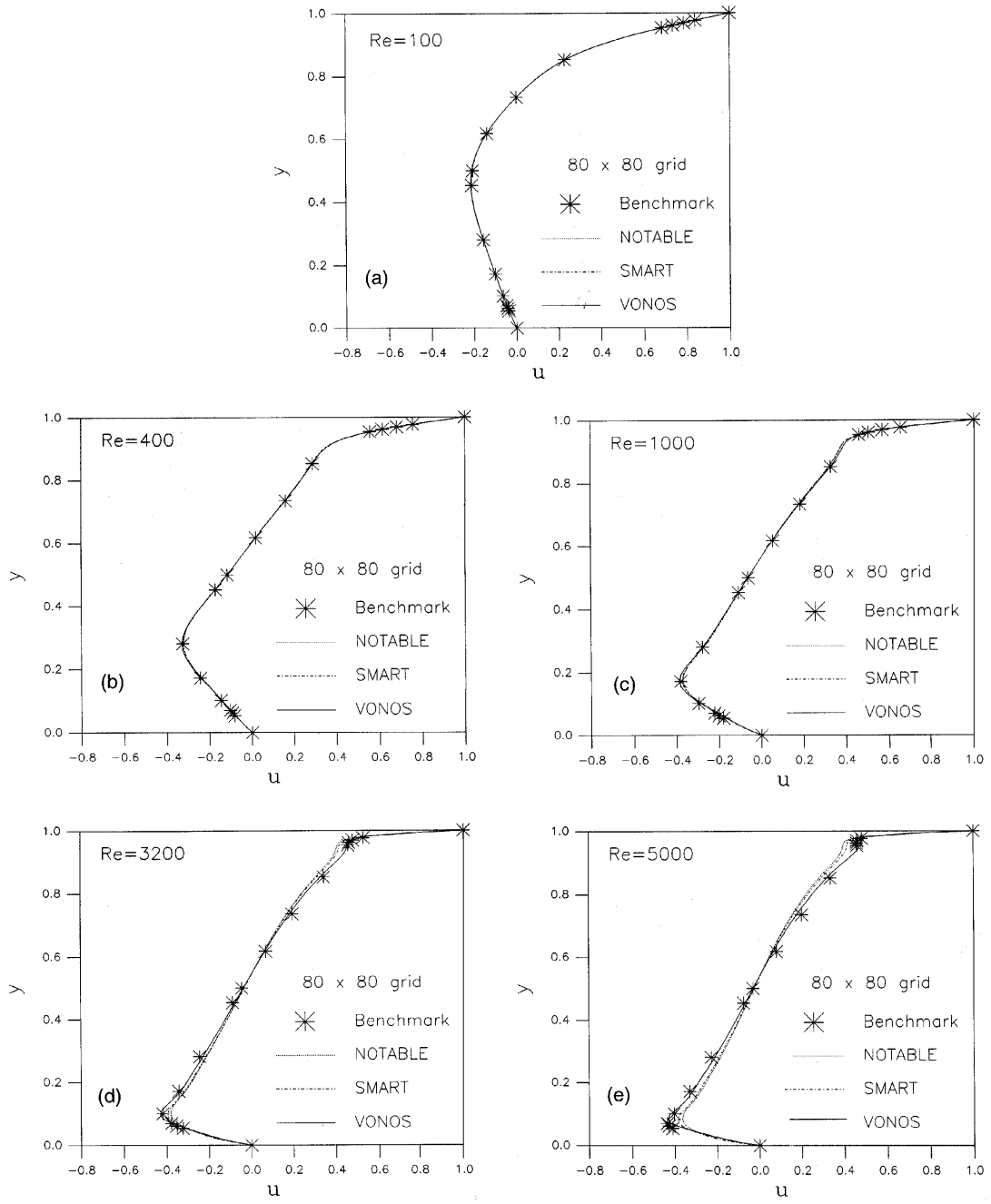


Figure 9. Comparison of $u$-velocity profiles along vertical centreline of cavity obtained with NOTABLE, SMART and VONOS ($80 \times 80$ grid) against benchmark solution for $Re =$ (a) 100, (b) 400, (c) 1000, (d) 3200 and (e) 5000

turbulence model on the solver convergence and the results accuracy. As the Reynolds number increases, the flow turns more and more convective, leading to convergence problems when unbounded schemes are used.

The Reynolds numbers tested in the present work were $Re = 100$, 400, 1000, 3200 and 5000. For NOTABLE, SMART and VONOS five runs for each Reynolds number were made using $20 \times 20$, $30 \times 30$, $40 \times 40$, $60 \times 60$ and $80 \times 80$ uniform grids. The SIMPLE algorithm was used in a collocated grid arrangement. The flow field was assumed converged when all normalized residuals were below $10^{-4}$. For all runs the underrelaxation factors used were 0·5 for both velocity and pressure. The same underrelaxation factor was used also for the source terms $SU_x$ and $SU_y$, except for $Re = 5000$ and the finer grids $60 \times 60$ and $80 \times 80$ where this factor was 0·1. The results are compared with the benchmark solution of Ghia *et al.*[9]

Figures 9(a)–9(e) present the velocity profiles at the geometric centre of the cavity for all Reynolds numbers using the $80 \times 80$ grid. It is clear that for low Reynolds numbers all predicted profiles coincide with the benchmark solution. This is valid also for the 'hybrid' scheme, as mentioned by Papadakis and Bergeles.[5] The differences of the solutions are visible for $Re > 3200$. For $Re = 5000$ there is a larger discrepancy between NOTABLE, SMART and VONOS. NOTABLE again gives the most diffusive solution and SMART fails to describe accurately the near-wall region. The advantage of using VONOS is better visible on coarser grids such as the $40 \times 40$ one.

The velocity profiles in Figure 10 show that when coarser grids are used, VONOS gives more accurate results than the other two schemes. This consideration is also proved by Figures 11 and 12.

Figure 11 shows the effect of grid refinement on the accuracy of the results. It is obvious that as the Reynolds number increases, VONOS has a superior performance compared with the other two schemes. For low Reynolds numbers NOTABLE and SMART are closer to the accuracy of VONOS. An important conclusion from this figure is that VONOS reaches practically a grid-independent solution as early as the $40 \times 40$ grid, especially for large Reynolds numbers.

Another important point is whether VONOS gives results of the same accuracy in less computational time than the other two schemes. Figure 12 gives the information concerning the CPU time used for the calculations. All computations were performed on a Power PC 604 processor. For all cases VONOS requires less computational time than NOTABLE and SMART. For low Reynolds numbers the computational time necessary for VONOS is the same as the time used by the other two

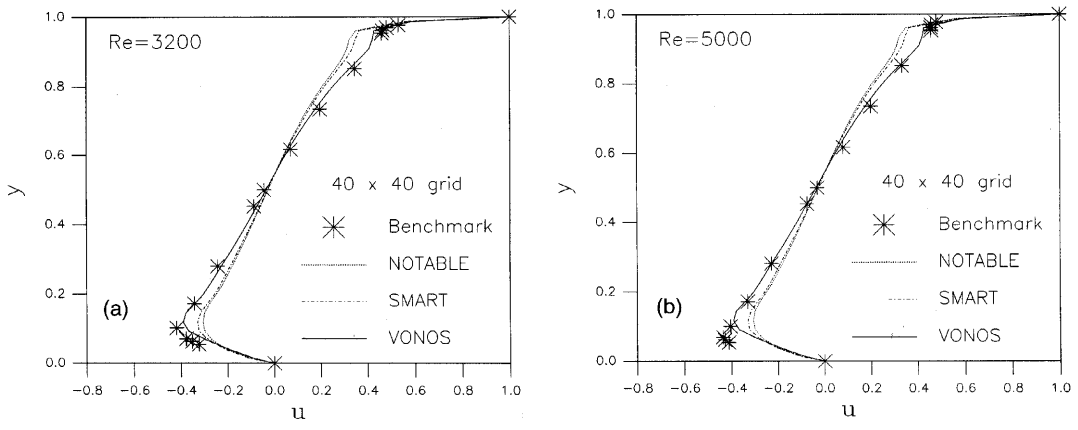


Figure 10. Comparison of $u$-velocity profiles along vertical centreline of cavity obtained with NOTABLE, SMART and VONOS ($40 \times 40$ grid) against benchmark solution for $Re =$ (a) 3200 and (b) 5000

 

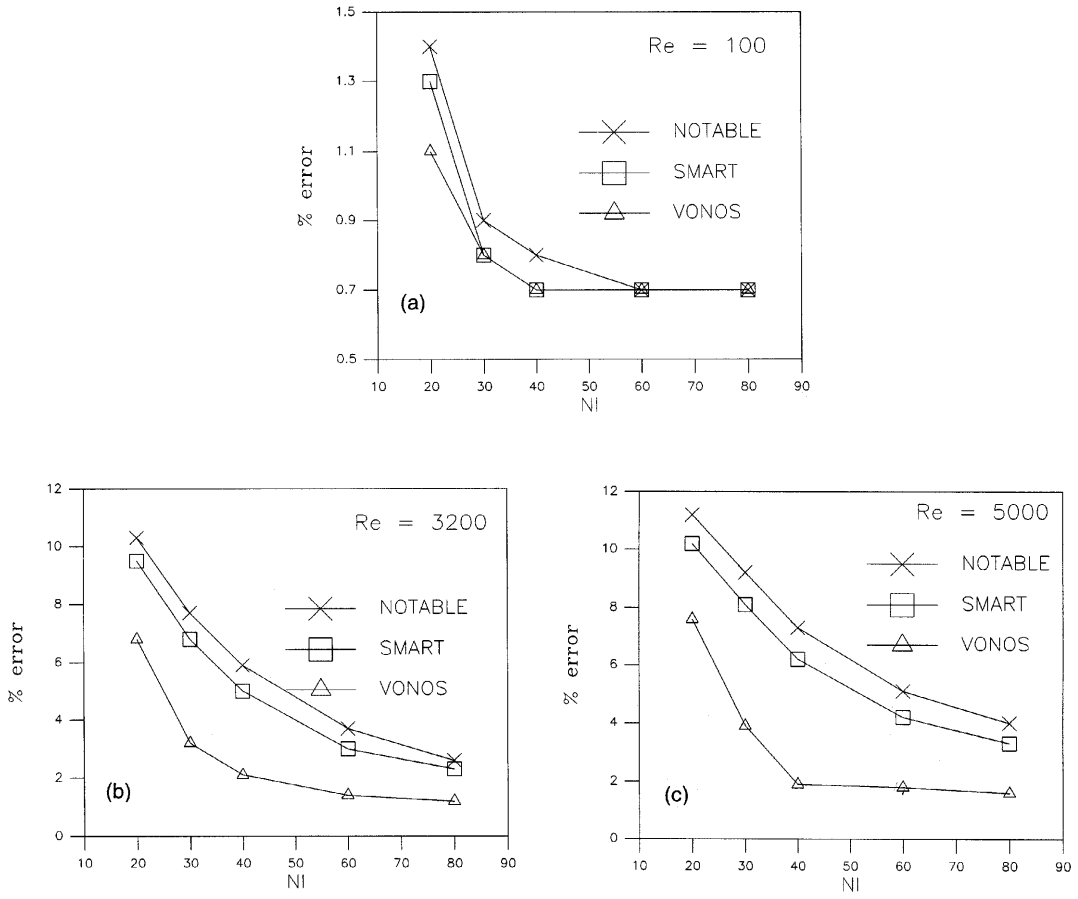


Figure 11. Effect of grid refinement on solution accuracy for NOTABLE, SMART and VONOS at $Re =$ (a) 100, (b) 3200 and (c) 5000

schemes. However, as the Reynolds number increases, the computational time for VONOS (for the same accuracy) is much less.

Table I presents a comparison of the primary vortex strength value with the benchmark value.[9] From this table it is deduced that in all cases VONOS gives the most accurate value. The value for $Re = 3200$, which is different from the benchmark value (vortex strength 0·1204), is very sensitive to small computational errors which are not associated with the velocity profile. Furthermore, as is clear in Figure 9, $Re = 3200$ is a transition value where the convective character of the flow becomes predominant.

Finally, Figure 14 presents the performance of NOTABLE, SMART and VONOS when a non-uniform ($20 \times 20$) grid is used. The grid is refined near the walls of the cavity and the non-uniformity is measured via the grid expansion ratio defined by

$$\lambda = \frac{\Delta x_{\mathrm{e-w}}}{\Delta x_{\mathrm{w-ww}}}. \tag{20}$$

From the predicted profiles it is clear that as the expansion ratio increases, VONOS comes closer to the benchmark solution.

 

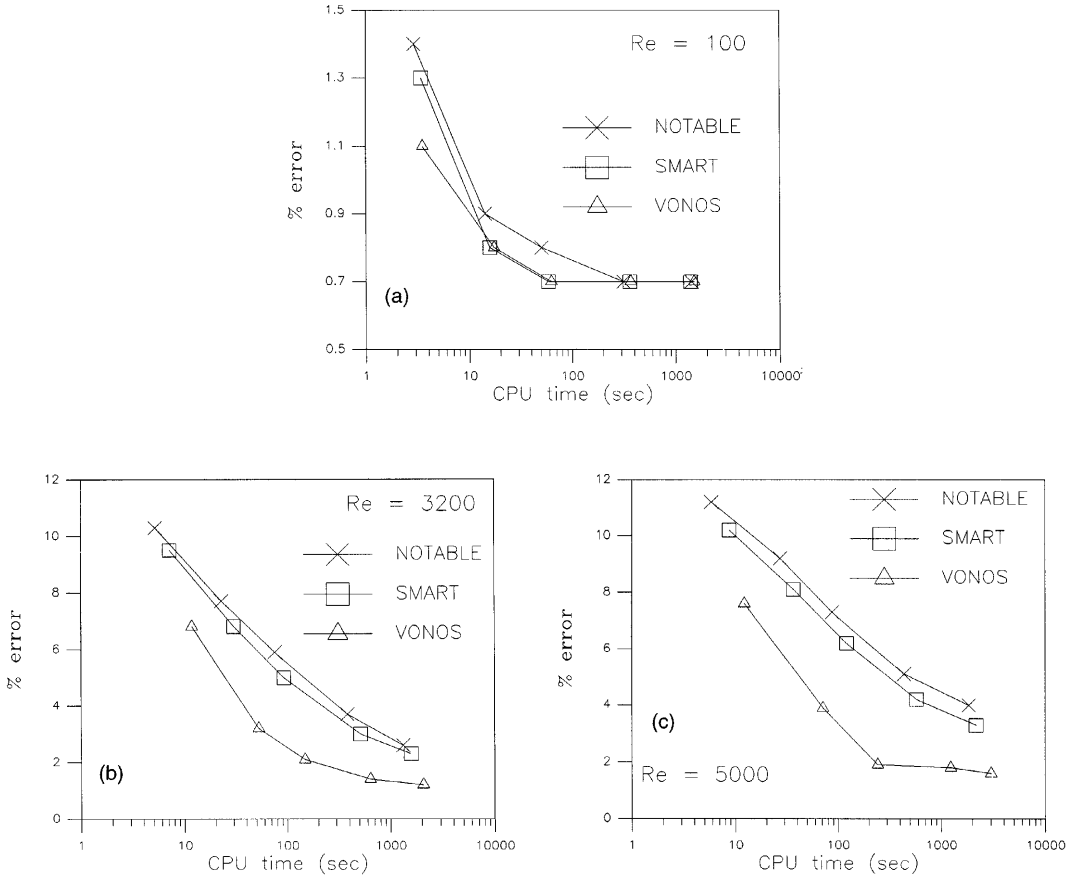


Figure 12. Accuracy as a function of required CPU time for NOTABLE, SMART and VONOS at $Re =$ (a) 100, (b) 3200 and (c) 5000

Table I. Strength of pimary vortex

| | $Re = 100$ | $Re = 400$ | $Re = 1000$ | $Re = 3200$ | $Re = 5000$ |
|---|---|---|---|---|---|
| NOTABLE | 0·1031 | 0·1125 | 0·1145 | 0·1075 | 0·0995 |
| SMART | 0·1031 | 0·1126 | 0·1149 | 0·1094 | 0·1029 |
| VONOS | 0·1032 | 0·1133 | 0·1167 | 0·1170 | 0·1189 |
| Benchmark | 0·1034 | 0·1139 | 0·1179 | 0·1204 | 0·1189 |

## 4. CONCLUSIONS

The development and assessment of a new scheme for convective modelling, called VONOS, proved that the scheme can be successfully implemented into the CFD computational codes. The scheme preserves the boundedness property and for that reason it can be used for every transport equation without giving stability problems. The performance of the scheme was tested in three test cases and is totally satisfactory, beyond the accuracy of formally third-order bounded schemes such as

 

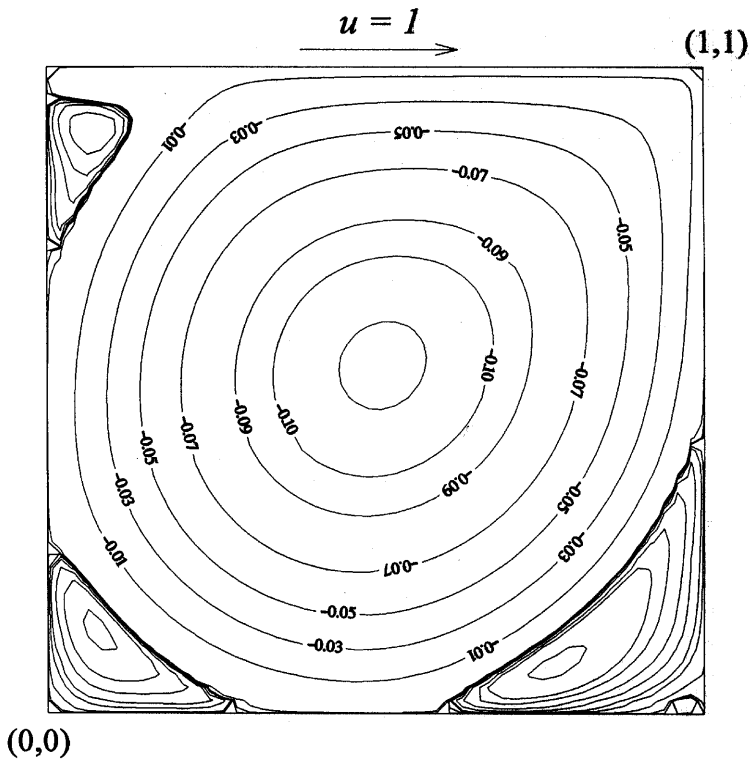


Figure 13. Streamlines in cavity: $Re = 5000$, VONOS scheme, $80 \times 80$ grid

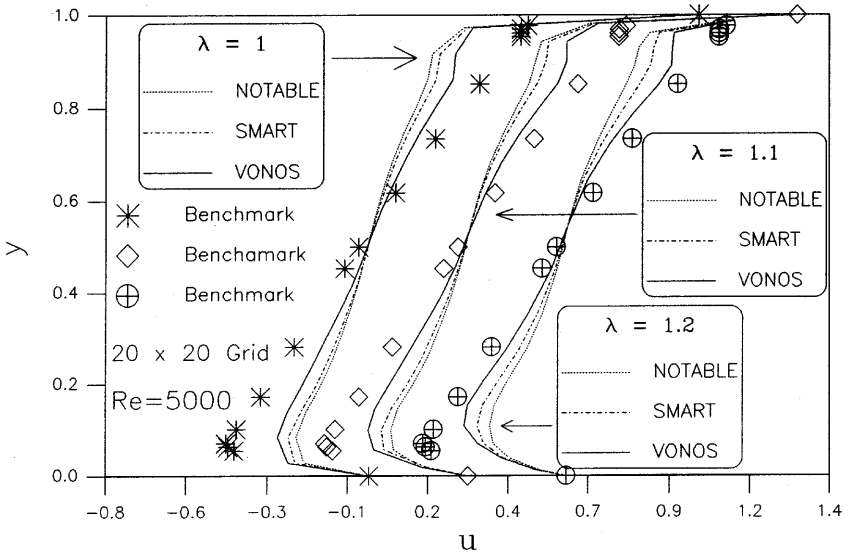


Figure 14. Comparison of $u$-velocity profiles along vertical centreline of cavity obtained with NOTABLE, SMART and VONOS against benchmark solution for $Re = 5000$ with $20 \times 20$ non-uniform grids

 

NOTABLE and SMART. Currently the scheme is used in a 3D code for the prediction of the flow and temperature field in coal-fired utility boilers.

ACKNOWLEDGEMENT

Part of this work has been supported by EU/DG XII, contract JOF-CT95-0005.

REFERENCES

1. B. P. Leonard and J. E. Drummond, 'Why you should not use ''hybrid'', ''Power-law'' or related exponential schemes for convective modeling—there are much better alternatives', *Int. j. numer. methods fluids*, **20**, 421–442 (1995).
2. B. P. Leonard, 'A stable and accurate convective modeling procedure based on quadratic interpolation', *Comput. Methods Appl. Mech. Eng.*, **19**, 59–98 (1979).
3. P. H. Gaskell and A. K. C. Lau, Curvature-compensated convective transport: SMART, a new boundedness-preserving transport algorithm', *Int. j. numer. methods fluids*, **8**, 617–641 (1988).
4. A. Pascau and C. Perez, 'A well-behaved scheme to model strong convection in a general transport equation', *Numer. Methods Lam. Turb. Flows*, **8**, 608–617 (1993).
5. G. Papadakis and G. Bergeles, 'A locally modified second order upwind scheme for convection terms discretized', *Int. J. Numer. Methods Heat Fluid Flow*, **5**, 49–62 (1995).
6. B. P. Leonard, 'The ULTIMATE conservative difference scheme applied to unsteady one-dimensional advection', *Comput. Methods Appl. Mech. Eng.*, **88**, 17–74 (1991).
7. B. P. Leonard and S. Mokhtari, 'Beyond first order upwinding: the ULTRA-SHARP alternative for non-oscillatory steady state simulation of convection', *Int. j. numer. methods eng.*, **30**, 729–766 (1990).
8. T. Hayase, J. A. Humphrey and R. A. Greif, 'A consistently formulated QUICK scheme for fast and stable convergence using finite-volume iterative calculation procedures', *J. Comput. Phys.*, **98**, 108–118 (1992).
9. U. Ghia, K. N. Ghia and C. T. Shin, 'High-Re solutions for incompressible flow using the Navier–Stokes equations and a multigrid method', *J. Comput. Phys.*, **48**, 387–411 (1982).
10. D. Yeh and G.-T. Yeh, 'Computer evaluation of high order numerical schemes to solve advective transport problems', *Comput. Fluids*, **24**, 919–929 (1995).

 